Cancer Immunotherapy Hot Paper

DOI: 10.1002/ange.201306866

Recruiting Cytotoxic T Cells to Folate-Receptor-Positive Cancer Cells**

*Sumith A. Kularatne, Vishal Deshmukh, Marco Gymnopoulos, Sandra L. Biroc, Jinming Xia, Shailaja Srinagesh, Ying Sun, Ning Zou, Mark Shimazu, Jason Pinkstaff, Semsi Ensari, Nick Knudsen, Anthony Manibusan, Jun Y. Axup, Chan Hyuk Kim, Vaughn V. Smider, Tsotne Javahishvili, and Peter G. Schultz**

One new class of biologics that is generating a great deal of interest as next-generation cancer therapeutics are bispecific antibodies that simultaneously target the cluster of differentiation 3 (CD3) protein and tumor-associated antigens to recruit cytotoxic T cells from the patient's own immune system to eliminate cancer cells.[1] Examples include the first approved bispecific antibody in Europe, Catumaxomab,[2] and Blinatumomab,[2] an anti-CD19-anti-CD3 bispecific antibody that showed a high rate of complete response in refractory acute lymphoblastic leukemia (ALL) patients in phase II clinical trials.[3,4] As cancer therapeutics, bispecific antibodies have several attractive features: formation of an immunological synapse results in efficient killing of tumor cells by activated T cells; T cell-mediated cytotoxicity can have a bystander effect on heterogeneous tumor and cancer stem cells; bispecific antibodies should be effective against cancers with upregulated drug pumps; and finally, bispecific antibodies do not rely on a high copy number of surface antigens or efficient receptor-mediated internalization.[5,6] In general, bispecific antibodies are expressed recombinantly as tandem ScFv or full-length chimeric antibodies,[7,8] but these constructs can suffer from poor pharmacokinetic and physical properties, immunogenicity, or manufacturing challenges.[9]

We recently developed a semisynthetic approach to the synthesis of bispecific antibodies using unnatural amino acids (UAAs) with orthogonal chemical reactivity that affords homogenous conjugates with precise control over the relative geometry of the two antibody binding sites. One such bispecific antibody that targets cytotoxic T cells to $Her2^+$ breast cancer cells showed good half-life and excellent efficacy in rodent xenograft models.[10] In addition to antibodies, small-molecule ligands have been identified with high affinity and specificity for tumor-associated cell-surface antigens.[11,12] One example is folic acid (FA), which binds tightly to the folate receptor (FR) and is highly expressed on a variety of cancer and inflammatory cells.[13] Based on the limited distribution of FR in healthy tissues, Low and coworkers have used folate for the selective delivery of antineoplastic agents to FR^+ cancers, such as ovarian cancer and non-small-cell lung cancer,[14] and these agents are showing promising clinical results. Although four isoforms of FR have been reported (FRα, FRβ, FRγ, and FRδ), only FRα and FRβ are overexpressed in epithelial-derived cancers (i.e., ovary, kidney, breast, liver), as well as anti- and pro-inflammatory macrophages.[15,16] Distribution of FRα in normal tissues is limited to the apical surfaces of the choroid plexus, the apical surfaces of proximal tubule cells of kidney, and in the airways of lungs.[17] Herein, we report the synthesis of a folate-derivatized anti-CD3 Fab conjugate (Figure 1 A) using UAA mutagenesis and show that it has excellent in vitro and in vivo activity.

Although FA consists of α- and γ-carboxylic acid groups, previous studies,[18] including a recent crystal structure of human folate receptor alpha in complex with folic acid,[19] indicates that its γ-carboxylic acid is solvent exposed and not involved in binding to FR, providing an ideal conjugation site for cytotoxic agents. Thus, a polar PEG linker was conjugated to the γ-carboxylic acid to improve the water solubility of FA, and to provide adequate distance for the formation of an immunological synapse between the cancer cells and T cells (Supporting Information, Scheme S1). An aminooxy moiety was incorporated at the distal end of the PEG linker and selectively conjugated by oxime bond formation (>95% yield) to an anti-human CD3 Fab fragment (UCHT1) with a genetically encoded *p*-acetylphenylalanine (pAcPhe) at position 136 in the heavy chain (HK136TAG), which is distal to the binding site. pAcPhe was site-specifically introduced into the Fab using an amber suppressor tRNA/aminoacyl-tRNA synthetase (aaRS) pair specific for pAcPhe (Figure S1A). The final conjugate was purified using a cation exchange column with a NaCl gradient at pH 6 and buffer exchanged into PBS (pH 7.4) to furnish the anti-CD3 Fab-folate conjugate in >95% yield. SDS-PAGE and mass spectrometry showed the expected mass with an approxi-

[*] Dr. S. A. Kularatne,[+] V. Deshmukh,[+] Dr. J. Y. Axup, Dr. C. H. Kim, Prof. V. V. Smider, Prof.Dr. P. G. Schultz
Department of Chemistry and The Skaggs Institute for Chemical Biology, The Scripps Research Institute
10550 North Torrey Pines Road, La Jolla, CA 92037 (USA)
E-mail: schultz@scripps.edu
Dr. M. Gymnopoulos,[+] Dr. S. L. Biroc, Dr. J. Xia, S. Srinagesh, Dr. Y. Sun, Dr. N. Zou, Dr. M. Shimazu, Dr. J. Pinkstaff, Dr. S. Ensari, N. Knudsen, A. Manibusan, Dr. T. Javahishvili
Ambrx Inc.
North Torrey Pines Road, La Jolla, CA 92037 (USA)
[+] These authors contributed equally to this work.

[**] This work was supported by the NIH grant R01 GM097206 (P.G.S.). This is manuscript 24012 of The Scripps Research Institute.

Supporting information for this article (including the synthesis of the anti-CD3 Fab-folate conjugate and other experimental procedures) is available on the WWW under http://dx.doi.org/10.1002/anie.201306866.

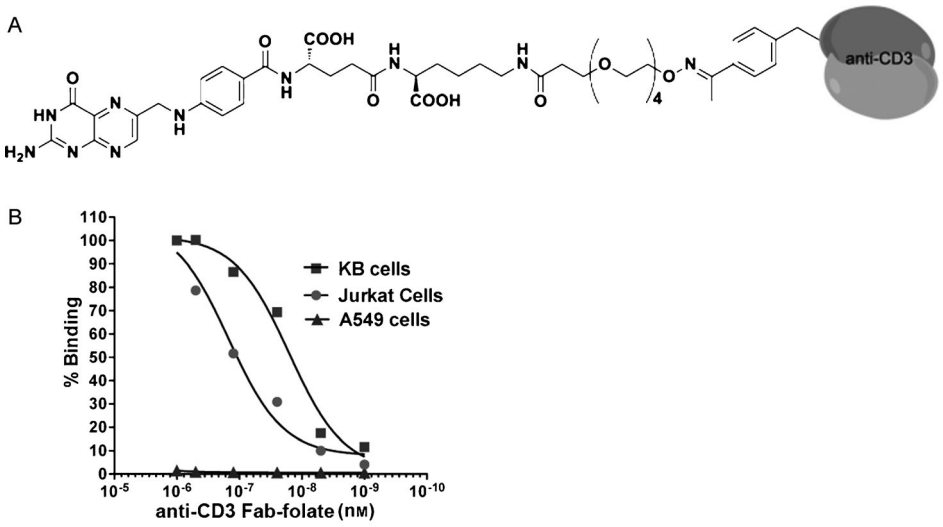

Figure 1. An anti-CD3 Fab-folate conjugate specific for FR and CD3. A) A folate/ethylene glycol linker was conjugated to anti-CD3 Fab. B) Dose-dependent binding of anti-CD3 Fab-folate to KB cells (FR^+) and Jurkat cells ($CD3^+$), but not to A549 cells (FR^-). Cells were incubated with increasing concentrations of the conjugate for 30 minutes at 4 °C and binding was analyzed by flow cytometry.

mately 813 Da difference between the anti-CD3 Fab-folate conjugate and the unconjugated anti-CD3 Fab, corresponding to conjugation of one folate per Fab (Figure S1B,C).

The affinity and specificity of the anti-CD3 Fab-folate conjugate were evaluated using both FR^+ and FR^- cell lines. After culture in folate-deficient media, FR was overexpressed in nasopharyngeal (KB) and ovarian (OV-90, SKOV-3) cancer cell lines as determined by flow cytometry (Figure S2). A kidney cancer cell line Caki-1 and an alveolar basal epithelial cell carcinoma A549 that did not express FR (Figure S2) were used as negative controls. The anti-CD3 Fab-folate conjugate was able to bind to KB cells (FR^+) with affinity similar to free folate (Figure 1B, Figure S3A), indicating minimal loss of binding to the folate receptor as a result of conjugation with the anti-CD3 Fab. Likewise, the anti-CD3 Fab-folate conjugate bound to Jurkat cells ($CD3^+$) with similar affinity to anti-CD3 (Figure 1B, Figure S3B); no binding was observed to A549 cells (FR^-) as expected (Figure 1B, Figure S3A).

We next tested the activity of the anti-CD3 Fab-folate conjugate in an in vitro cytotoxicity assay with KB and OV-90 cells (FR^+), using Caki-1 and A549 cells (FR^-) as controls. Cells were co-cultured with activated human peripheral blood mononuclear cells (PBMCs; 1:10 ratio of target/effector cells) and treated with various concentrations of anti-CD3 Fab-folate or anti-CD3 Fab alone. Cytotoxicity was quantitated by measuring released lactate dehydrogenase (LDH) levels from lysed cells and with CellTiter-Glo and flow-cytometry-based toxicity assays. The anti-CD3 Fab-folate conjugate demonstrated efficient killing of KB and OV-90 cells in the presence of PBMCs with EC_{50} values of 10 pM and 100 pM, respectively (Figure 2A, Figure S4), while Caki-1 cells (Figure 2A) and A549 cells (Figure S4) were unaffected by 100 nM of the conjugate. Treatment with anti-CD3 Fab alone induced negligible toxicity on all cell lines tested (Figure 2A). Furthermore, incubation (16 hours) of SKOV-3 cells (Figure 2B) or KB cells (Figure S5) with activated PBMCs (1:10 ratio of target/effector cells) in folate-deficient media in the presence of the anti-CD3 Fab-folate conjugate resulted in the formation of rosettes, providing additional evidence for T cell targeting. In contrast, the anti-CD3 Fab had no effect on T cell engagement and clusters were not observed in the absence of PBMCs or KB cells (Figure S5).

We next examined the pharmacokinetics (PK) of the anti-CD3 Fab-folate conjugate and the unconjugated anti-CD3 Fab in rodents. A single dose of 1 mg kg^{-1} or 5 mg kg^{-1} of anti-CD3 Fab-folate in PBS or 1 mg kg^{-1} unconjugated anti-CD3 Fab was injected intravenously in three rats, serum was collected at regular intervals and analyzed by ELISA. The serum concentration decreased for both the anti-CD3 Fab-folate conjugate and the corresponding unconjugated mutant anti-CD3 Fab at the same rate with a serum half-life of

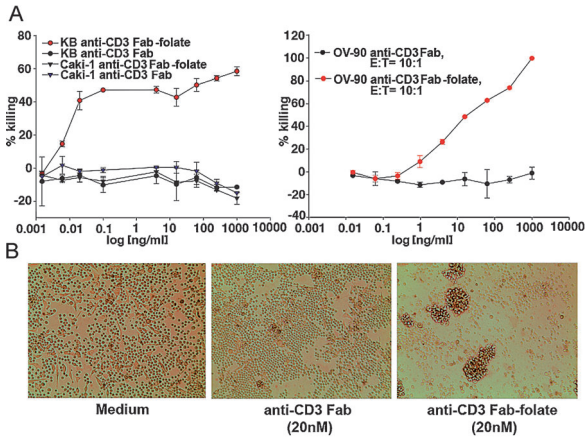

Figure 2. T cell engagement of target cells and dose-dependent toxicity of the anti-CD3 Fab-folate conjugate. A) Dose-dependent T cell-mediated cytotoxicity with KB (FR^+), OV-90 (FR^+), and Caki-1 (FR^-) cells treated with anti-CD3 Fab-folate in the presence of activated human PBMCs (1:10 ratio of target/effector cells). Increasing concentrations of anti-CD3 Fab-folate or unconjugated anti-CD3 Fab were incubated with target cells for 12–24 h at 37 °C and 5% CO_2. Cytotoxicity was quantitated by measuring LDH levels released from lysed cells according to the manufacturer's protocol (Cytotox 96 nonradioactive cytotoxicity assay, Promega). B) SKOV-3 cells were maintained in folate-free RPMI-1640 medium supplemented with 10% FBS for at least three passages before being seeded in a 48-well cell-culture plate and allowed to attach to the plate, after which activated human PBMCs (1:10 ratio of target/effector cells) were added. Anti-CD3 Fab or anti-CD3 Fab-folate was diluted in folate-free medium and added at the indicated concentration and the co-culture was incubated for 16 h. Images were taken with a VistaVision microscope with a 25× objective.

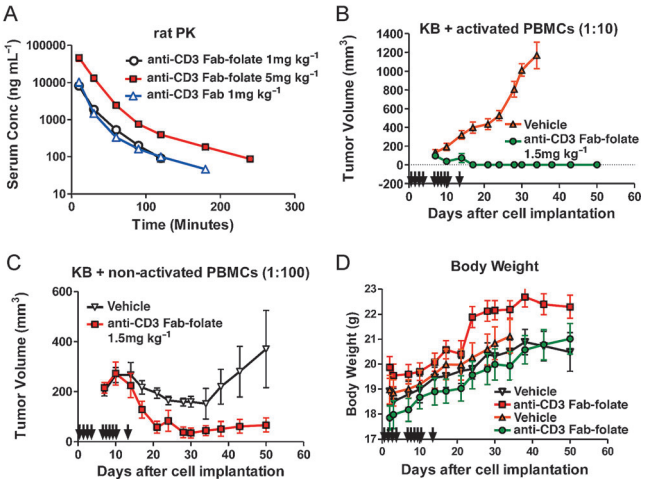

Figure 3. In vivo efficacy studies of anti-CD3 Fab-folate. A) The serum half-life of anti-CD3 Fab-folate was measured after a single bolus IV injection of male Sprague Dawley rats. NOD-SCID mice bearing KB tumors co-implanted with B) human-activated PBMCs 1:10 ratio (target/effector) or C) non-activated PBMCs 1:100 ratio (target/effector; $N = 10$ mice per group). Animals were treated intravenously with 1.5 mg kg^{-1} anti-CD3 Fab-folate or vehicle daily for ten injections (black arrows) starting on the same day as tumor cell implantation. Tumors were measured in two perpendicular directions and their volumes were estimated using the formula $V = (L \times W \times W)/2$ where V = volume, W = shortest diameter, and L = longest diameter. Body weight D) does not decrease during the dosing period suggesting the material is not overtly toxic. Data points represent the group average and error bars represent the standard error of the mean.

60 minutes (Figure 3A). Thus, the anti-CD3 Fab-folate conjugate has similar pharmacokinetics to the unconjugated anti-CD3 Fab, indicating that PK profile of the conjugate was not affected by folate modification.

The in vivo efficacy of the anti-CD3 Fab-folate bispecific agent was then assessed in a xenograft model using female NOD-SCID mice. Animals were maintained on a low-folate diet to reduce circulating serum levels of folate that might compete with the bispecific agent (in a clinical context, patients could also be prescribed a restricted folate diet prior to therapy). Because the number and activation status of effector T cells in a cancer patient is not well understood, we chose to investigate the efficacy of the anti-CD3 Fab-folate conjugate with varying numbers of both non-activated as well as activated human PBMCs. KB (FR$^+$) or A549 (FR$^-$) cells were able to form tumors when mixed with non-activated human PBMCs (1:100 ratio of target/effector cells) or activated human PBMCs (1:10 ratio of target/effector cells) and injected subcutaneously into mice. We therefore implanted KB cells mixed with activated human PBMCs (1:10 ratio of target/effector cells) into mice and injected the mice intravenously with 1.5 mg kg^{-1} of anti-CD3 Fab-folate or PBS daily for ten days starting on the same day as the tumor cell implantation. This dosing regimen was chosen based on the pharmokinetic properties of the anti-CD3 Fab-folate conjugate and previous studies with bispecific antibodies.[10] Tumor volumes showed a rapid increase in the PBS-treated mice, with a doubling time of approximately five days. In contrast, tumors in mice treated with anti-CD3 Fab-folate were barely detectable throughout the duration of the study (Figure 3B). In a parallel study, mice were implanted with KB cells mixed with unactivated human PBMCs (1:100 ratio of target/effector cells) and treated intravenously with 1.5 mg kg^{-1} of anti-CD3 Fab-folate or PBS daily for ten days starting on the same day as tumor cell implantation. Tumor volumes for both groups of mice decreased for the first 30 days of the study, possibly owing to the high burden of PBMCs at the injection site. The rate of decease of the tumors was, however, higher in the anti-CD3 Fab-folate-treated mice. After day 35 of the study, the tumors in PBS-treated mice steadily increased in volume while tumors in the anti-CD3 Fab-folate-treated mice decreased to barely detectable levels, indicating the engagement of cytotoxic T cells for the elimination of the tumors by the anti-CD3 Fab-folate conjugate even in the absence of activated T cells (Figure 3C). To test the in vivo selectivity of the anti-CD3 Fab-folate conjugate for FR expressing tumors, A549 cells (FR$^-$) were mixed with unactivated human PBMCs (1:100 ratio of target/effector cells) and implanted in mice. Mice were treated in a similar manner with ten daily intravenous doses of 1.5 mg kg^{-1} anti-CD3 Fab-folate and showed no significant difference from PBS-treated tumors 20 days after treatment (Figure S6A). Throughout all these studies no weight loss or other overt toxicity was observed in both anti-CD3 Fab-folate and PBS-treated mice (Figure 3D, Figure S6B). We further performed histopathological analysis of the mice both with and without anti-CD3 Fab-folate injection. Staining of kidneys from mice treated with anti-CD3 Fab-folate or PBS showed no infiltration of T cells; no obvious pathological differences in hematoxylin and eosin (H&E) staining between the treatment and control groups were observed for other tissues such as spleen, lung, and liver (Figure S7).

We have developed a simple, high-yield method for the conjugation of folate to an anti-CD3 Fab to afford chemically defined, ligand-targeted anti-CD3 antibodies. This anti-CD3 Fab-folate conjugate was able to engage human PBMCs in vitro and in vivo to mediate the lysis of FR$^+$ tumor cells. Recently, an anti-CD3 Fab-folate conjugate was synthesized using a selenocysteine Fab mutant.[20] This conjugation strategy, however, involves the formation of a maleimide linkage, which is relatively unstable at physiological pH, is limited to substitution near the C-terminus, and affords relatively low yields of the isolated product. A complementary approach targets FR$^+$ tumors using folic acid to deliver the chemotherapeutic drug, vinblastine, and is currently being evaluated in the clinic against platinum-resistant ovarian cancer and non-small-cell lung cancer,[21,22] The results presented herein not only further emphasize the utility of targeting high-affinity FR on the cell surface of tumors, but also provide a general method for site-specific conjugation of targeting ligands to antibodies with a high degree of control over conjugation site and stoichiometry. We are currently extending this approach to other tumor-specific ligands as well as other effector domains.

Received: August 5, 2013
Published online: September 25, 2013

Keywords: bispecific antibody · cancer · folate receptor · immunotherapy · T cells

[1] P. Chames, D. Baty, *mAbs* **2009**, *1*, 539 – 547.
[2] D. Nagorsen, P. Kufer, P. A. Baeuerle, R. Bargou, *Pharmacol. Ther.* **2012**, *136*, 334 – 342.
[3] M. S. Topp et al., *J. Clin. Oncol.* **2011**, *29*, 2493 – 2498.
[4] M. S. Topp et al., *Blood* **2012**, *120*, 5185 – 5187.
[5] A. B. van Spriel, H. H. van Ojik, J. G. van De Winkel, *Immunol. Today* **2000**, *21*, 391 – 397.
[6] Y. Cao, L. Lam, *Adv. Drug Delivery Rev.* **2003**, *55*, 171 – 197.
[7] L. Presta, *Curr. Opin. Struct. Biol.* **2003**, *13*, 519 – 525.
[8] J. Kriangkum, B. Xu, L. P. Nagata, R. E. Fulton, M. R. Suresh, *Biomol. Eng.* **2001**, *18*, 31 – 40.
[9] P. Chames, M. Van Regenmortel, E. Weiss, D. Baty, *Br. J. Pharmacol.* **2009**, *157*, 220 – 233.
[10] C. H. Kim, J. Y. Axup, A. Dubrovska, S. A. Kazane, B. A. Hutchins, E. D. Wold, V. V. Smider, P. G. Schultz, *J. Am. Chem. Soc.* **2012**, *134*, 9918 – 9921.
[11] K. F. Becker, H. Höfler, *Curr. Cancer Drug Targets* **2001**, *1*, 121 – 128.
[12] O. M. Fischer, A. Gschwind, A. A. Ullrich, *Discovery Med.* **2004**, *4*, 166 – 171.
[13] J. Sudimack, R. J. Lee, *Adv. Drug Delivery Rev.* **2000**, *41*, 147 – 162.
[14] Y. Lu, E. Sega, C. P. Leamon, P. S. Low, *Adv. Drug Delivery Rev.* **2004**, *56*, 1161 – 1176.
[15] A. Puig-Kröger, E. Sierra-Filardi, A. Domínguez-Soto, R. Samaniego, M. T. Corcuera, F. Gómez-Aguado, M. Ratnam, P. Sánchez-Mateos, A. L. Corbí, *Cancer Res.* **2009**, *69*, 9395 – 9403.
[16] M. D. Salazar, M. Ratnam, *Cancer Metastasis Rev.* **2007**, *26*, 141 – 152.
[17] M. Wu, W. Gunning, M. Ratnam, *Cancer Epidemiol. Biomarkers Prev.* **1999**, *8*, 775 – 782.
[18] S.-L. Kim, H.-J. Jeong, E.-M. Kim, C.-M. Lee, T.-H. Kwon, M.-H. Sohn, *J. Korean Med. Sci.* **2007**, *22*, 405 – 411.
[19] C. Chen, J. Ke, X. E. Zhou, W. Yi, J. S. Brunzelle, J. Li, E.-L. Yong, H. E. Xu, K. Melcher, *Nature* **2013**, *500*, 486 – 489.
[20] H. Cui, J. D. Thomas, T. R. Burke, C. Rader, *J. Biol. Chem.* **2012**, *287*, 28206 – 28214.
[21] P. M. Lorusso et al., *J. Clin. Oncol.* **2012**, *30*, 4011 – 4016.
[22] M. J. Edelman, W. A. Harb, S. E. Pal, R. V. Boccia, M. J. Kraut, P. Bonomi, B. A. Conley, J. S. Rogers, R. A. Messmann, E. B. Garon, *J. Thorac. Oncol.* **2012**, *7*, 1618 – 1621.